

Effects of high-dose Mn implantation into ZnO grown on sapphire

Y. W. Heo, M. P. Ivill, K. Ip, D. P. Norton, and S. J. Pearton^{a)}

Department of Materials Science and Engineering, University of Florida, Gainesville, Florida 32611

J. G. Kelly, R. Rairigh, and A. F. Hebard

Department of Physics, University of Florida, Gainesville, Florida 32611

T. Steiner

Air Force Office of Scientific Research, Arlington, Virginia 22217

(Received 4 December 2003; accepted 28 January 2004)

ZnO films grown by pulsed-laser deposition on *c*-plane Al₂O₃ substrates were annealed at temperatures up to 600 °C to produce *n*-type carrier concentrations in the range 7.5×10^{15} – 1.5×10^{20} cm⁻³. After high-dose (3×10^{16} cm⁻²) Mn implantation and subsequent annealing at 600 °C, all the films show *n*-type carrier concentrations in the range 2 – 5×10^{20} cm⁻³ and room temperature hysteresis in magnetization loops. The saturation magnetization and coercivity of the implanted single-phase films were both strong functions of the initial anneal temperature, suggesting that carrier concentration alone cannot account for the magnetic properties of ZnO:Mn, and that factors such as crystalline quality and residual defects play a role. © 2004 American Institute of Physics. [DOI: 10.1063/1.1690111]

The properties of ZnO make it an attractive candidate for UV light-emitters, varistors, transparent high-power electronics, surface acoustic wave devices, piezoelectric transducers, gas-sensing, window material for flat-panel displays, and more efficient solar cells.^{1–12} There is also interest in developing the use of ion implantation of ZnO for device doping and isolation,⁸ as well as investigating the effectiveness of different transition metals for magnetic doping. The model by Dietl *et al.*^{13,14} predicts that the transition temperature in dilute magnetic semiconductors (DMSs) will scale with a reduction in the atomic mass of the constituent elements due to an increase in *p*–*d* hybridization and a reduction in spin–orbit coupling. The theory predicts a *T*_C greater than 300 K for *p*-type ZnO, with *T*_C dependent on the concentration of magnetic ions and holes. Ferromagnetism (FM) in magnetically doped ZnO has also been theoretically investigated by *ab initio* calculations based on local density approximation.^{15,16} The results suggest that FM ordering of Mn is favored when mediated by hole doping. However, for V, Cr, Fe, Co, and Ni dopants, FM ordering in ZnO is predicted to occur without the need of additional charge carriers. FM has been observed in *n*-type Mn-implanted, Sn-doped ZnO crystals,¹⁷ where Sn is a doubly ionized donor impurity. The Curie temperature is quite high, approaching 250 K. The Sn may simply provide carriers, albeit electrons, which effectively mediate the spin interactions or which could alternatively form complexes with Mn, resulting in both Mn⁺² and Mn⁺³ sites that could yield a ferrimagnetic ordering. Several groups have investigated the magnetic properties of TM-doped ZnO. In all of these studies, the ZnO material was *n*-type and shows either spin-glass,¹⁸ paramagnetic,^{19,20} or FM behavior.^{21–23} In Ni-doped ZnO thin films doped with 3 to 25 at. % Ni, FM was observed at 2 K with superparamagnetism above 30 K,²⁴ while FM has been reported for Co or

Fe doping.^{25–27} Despite the uncertainty in the mechanism, these results (high temperature ferromagnetism in Co- and Mn,Sn-doped ZnO) indicate a pathway for exploring spintronics in ZnO materials. The ionic radius of Mn⁺² (0.66 Å) is relative close to that for Zn (0.60 Å), suggesting moderate solid solubility without phase segregation. As such, the primary transition metal dopant of interest will be Mn. Chromium and cobalt also present the possibility of achieving FM in ZnO via doping with magnetic ions for which the net superexchange coupling is FM.

In this letter, we report on the effects of initial carrier concentration in thin films of ZnO deposited on sapphire on the resulting transport and magnetic properties after high dose Mn implantation and annealing.

The phosphorus-doped ZnO epitaxial films in this study were grown by pulsed-laser deposition (PLD) on single-crystal (0001) Al₂O₃ substrate, using a ZnO:P_{0.02} target and a KrF excimer laser ablation source.²⁸ The laser repetition rate and laser pulse energy density were 1 Hz and 3 J cm⁻², respectively. The films were grown at 400 °C in an oxygen pressure of 20 mTorr. The samples were annealed in the PLD chamber at temperatures ranging from 425 to 600 °C in O₂ ambient (100 mTorr) for 60 min. The resulting film thickness ranged from 350 to 500 nm. Four-point van der Pauw Hall measurements were performed to obtain the carrier concentration and mobility in the films. The carrier concentrations ranged from 7.5×10^{15} to 1.5×10^{20} cm⁻³, with corresponding mobilities in the range 16–6 cm²/V s, as shown in Fig. 1.

The films were implanted with 250 keV Mn⁺ ions to a dose of 3×10^{16} cm⁻² with the samples held at ~300 °C to avoid amorphization and subsequently annealed at 600 °C for 1 min in air in a Heatpulse 610 T system. The transport properties were again obtained from Hall measurements and are also shown in Fig. 1. The carrier concentration was in the range 2 – 5×10^{20} in each case with electron mobilities of 15–23 cm²/V s. The high electron concentration could arise

^{a)}Electronic mail: spear@mse.ufl.edu

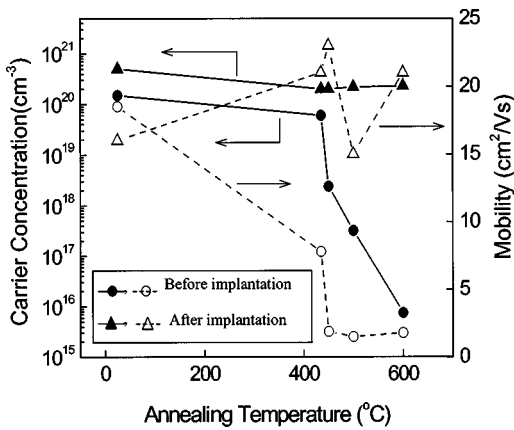


FIG. 1. Carrier concentration and electron mobility in *n*-type, P-doped ZnO films after annealing at different temperatures and after the same films were then implanted with Mn and annealed at a fixed temperature of 600 °C.

from residual implant damage or formation of Mn-related donor complexes. It is clear that the transport properties are dominated by these effects since in each case, the carrier concentration is significantly larger than in the samples prior to implantation.

The magnetic properties were obtained using a commercially available rf-superconducting quantum interface device (Quantum Design MPMS). None of the films showed any evidence for second-phase formation from x-ray diffraction measurements. In each case, the Mn-implanted samples showed differences in field-cooled (FC) and zero-field-cooled (ZFC) magnetization out to at least room temperature. An example is shown in Fig. 2 for the sample that was not annealed prior to implantation. The difference between the two plots advantageously eliminates para- and diamagnetic contributions and indicates the presence of hysteresis if the difference is nonzero. This is particularly advantageous for thin-film samples, in which the amount of FM material in unoptimized samples may be small. For samples that have hysteresis that extends higher than the highest temperature we reach in the FC-ZFC measurement, the FC-ZFC results do not have a well-defined meaning, and hysteresis can still be observed at temperatures higher than the point at which the difference goes to zero. Although FM is the usual explanation for hysteresis, spin-glass effects, cooperative interactions between superparamagnetic clusters, or superparamagnetism below a blocking temperature can also be the cause.

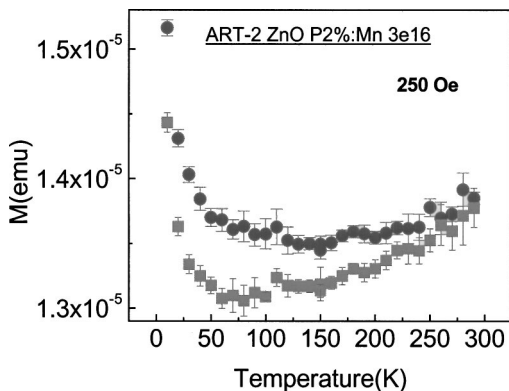


FIG. 2. Temperature dependence of FC (circles) and ZFC (squares) magnetization in Mn-implanted ZnO subsequently annealed at 600 °C.

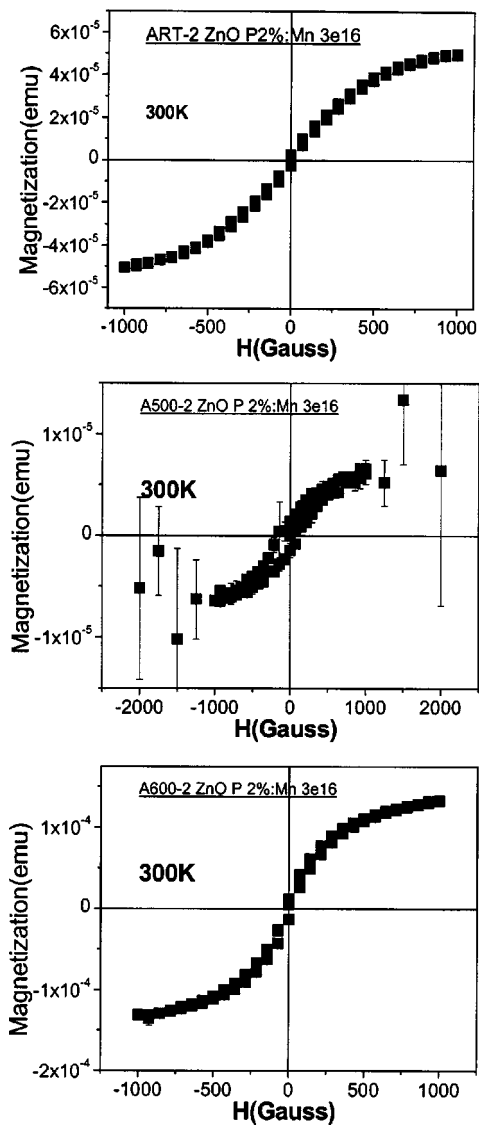


FIG. 3. Magnetization versus field at 300 K for different films of ZnO implanted with Mn and subsequently annealed at 600 °C. The sample at top was not annealed after growth, the one at center was annealed at 500 °C, and the one at bottom was annealed at 600 °C after growth.

The FC magnetization shows a positive curvature with a pronounced upturn at low temperatures. These rather unconventional shapes in the temperature-dependent magnetization were first seen in (Ga,Mn)As²⁹ and seem to be the rule rather than the exception in most DMS materials. Possible explanations for this behavior can be found in theoretical treatments that consider the effect of randomness and disorder on percolating FM clusters.^{30–32}

Figure 3 shows the hysteresis in 300 K magnetization versus field plots for three different samples after Mn implantation and annealing at 600 °C. There is a remarkable change in both the saturation magnetization and coercivity for these samples implanted under identical conditions, even though the final electrical properties are almost the same. This is a strong indication that carrier concentration alone is not the only parameter that influences the magnetic characteristics of the ZnO:Mn. This is consistent with the work of Theodoropoulou *et al.*,²³ who found that FM in ZnO thin films deposited by reactive magnetron sputtering was strongly dependent on parameters such as growth tempera-

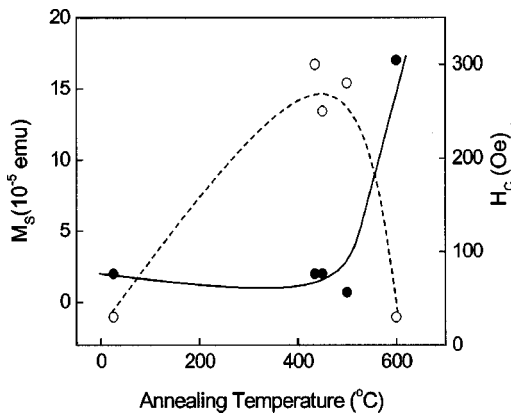


FIG. 4. Saturation magnetization (closed circles) and coercivity (open circles) of ZnO films annealed at various temperatures after growth, and then implanted with Mn and subsequently annealed at 600 °C.

ture, O₂ partial pressure, and type of substrate (only films deposited on Al₂O₃ substrates were FM). Nonoptimized growth conditions produced weakly paramagnetic behavior.²³

Figure 4 shows the dependence of room temperature saturation magnetization (M_S) and coercivity (H_C) on the initial post-growth annealing temperature of the ZnO films. The highest M_S values were obtained for the sample annealed initially at 600 °C, which is likely to have the best crystalline quality and which had the lowest electron concentration. This may lead to a more even distribution of substitutional Mn²⁺, minimizing antiferromagnetic coupling.²³ In the *ab initio* calculations of Refs. 15 and 16, hole doping stabilizes the FM state in Mn-doped ZnO, and the spin-glass state becomes more energetic favorable as the *n*-type doping increases.

In conclusion, high-dose Mn implantation into ZnO thin films grown on sapphire substrates produces ferromagnetism for all *n*-type doping levels investigated. The saturation magnetization is a strong function of the initial electrical properties of the films prior to implantation and explains some of the variation in magnetic properties reported in the literature for films grown by different methods on different substrates.

The work at UF is partially supported by AFOSR grant under grant no. F49620-03-1-0370.

- ¹H. Hayashi, A. Ishizaka, M. Haemori, and H. Koinuma, Appl. Phys. Lett. **82**, 1365 (2003).
- ²P. Sharma, K. Sreenivas, and K. V. Rao, J. Appl. Phys. **93**, 3963 (2003).
- ³J. S. Horwitz, W. H. Kim, A. J. Mäkinen, Z. H. Kafafi, and D. B. Chrisey, Thin Solid Films **420–421**, 539 (2002).
- ⁴D. C. Look, Mater. Sci. Eng., B **80**, 383 (2001).
- ⁵M. Wraback, H. Shen, S. Liang, C. R. Gorla, and Y. Lu, Appl. Phys. Lett. **74**, 507 (1999).
- ⁶D. C. Look, J. W. Hemsky, and J. R. Sizelove, Phys. Rev. Lett. **82**, 2552 (1999).
- ⁷F. D. Auret, S. A. Goodman, M. Hayes, M. J. Legodi, H. A. van Laarhoven, and D. C. Look, Appl. Phys. Lett. **80**, 956 (2002).
- ⁸S. O. Kucheyev, J. E. Bradley, J. S. Williams, C. Jagerdish, and M. V. Swain, Appl. Phys. Lett. **80**, 956 (2002).
- ⁹M. Wraback, H. Shen, S. Liang, C. R. Gorla, and Y. Lu, Appl. Phys. Lett. **76**, 507 (1999).
- ¹⁰T. Aoki, D. C. Look, and Y. Hatanaka, Appl. Phys. Lett. **76**, 3257 (2000).
- ¹¹C. R. Gorla, N. W. Emanetoglu, S. Liang, W. E. Mayo, Y. Lu, M. Wraback, and H. Shen, J. Appl. Phys. **85**, 2595 (1999).
- ¹²S. Krishnamoorthy, A. A. Iliadis, A. Inumpudi, S. Choopun, R. D. Vispute, and T. Venkatesan, Solid-State Electron. **46**, 1631 (2002).
- ¹³T. Dietl, H. Ohno, F. Matsukura, J. Cibert, and D. Ferrand, Science **287**, 1019 (2000).
- ¹⁴T. Dietl, Semicond. Sci. Technol. **17**, 377 (2002).
- ¹⁵K. Sato and H. Katayama-Yoshida, Jpn. J. Appl. Phys. **39**, L555 (2000).
- ¹⁶K. Sato and H. Katayama-Yoshida, Semicond. Sci. Technol. **17**, 367 (2002).
- ¹⁷D. P. Norton, S. J. Pearton, A. F. Hebard, N. Theodoropoulou, L. A. Boatner, and R. G. Wilson, Appl. Phys. Lett. **82**, 239 (2003).
- ¹⁸T. Fukumura, Z. Jin, A. Ohtomo, H. Koinuma, and M. Kawasaki, Appl. Phys. Lett. **78**, 958 (2001).
- ¹⁹A. Tiwari, C. Jin, A. Kvit, D. Kumar, J. F. Muth, and J. Narayan, Solid State Commun. **121**, 371 (2002).
- ²⁰S.-J. Han, T. H. Jang, Y. B. Kim, B. G. Park, J. H. Park, and Y. H. Jeong, Appl. Phys. Lett. **83**, 920 (2003).
- ²¹S. W. Jung, S.-J. An, G.-C. Yi, C. U. Jung, S.-I. Lee, and S. Cho, Appl. Phys. Lett. **80**, 4561 (2002).
- ²²P. Sharma, A. Gupta, K. V. Rao, F. J. Owens, R. Sharma, R. Ahuja, J. M. Osorio Guillen, B. Johansson, and G. A. Gehring, Nat. Mater. **2**, 673 (2003).
- ²³N. Theodoropoulou, G. P. Berera, V. Misra, P. LeCalir, J. Philip, J. S. Moodera, B. Satapi, and T. Som (unpublished).
- ²⁴T. Wakano, N. Fujimura, Y. Morinaga, N. Abe, A. Ashida, and T. Ito, Physica C **10**, 260 (2001).
- ²⁵W. Prellier, A. Foucheta, and B. Mercey, J. Phys. C **15**, R1583 (2003).
- ²⁶K. Rode, A. Anane, R. Mattana, J. P. Contour, O. Durand, and R. Lebourgeois, J. Appl. Phys. **93**, 7676 (2003).
- ²⁷S. J. Han, J. W. Song, C. H. Yang, S. H. Park, J. H. Park, Y. H. Jeong, and K. W. Rhie, Appl. Phys. Lett. **81**, 4212 (2002).
- ²⁸Y. W. Heo, S. J. Park, K. Ip, S. J. Pearton, and D. P. Norton, Appl. Phys. Lett. **83**, 1128 (2003).
- ²⁹H. Ohno, A. Shen, F. Matsukura, A. Oiwa, A. Endo, S. Katsumoto, and Y. Iye, Appl. Phys. Lett. **69**, 363 (1996).
- ³⁰M. Berciu and R. Bhatt, Phys. Rev. Lett. **87**, 107203.1 (2001).
- ³¹M. Mayr, G. Alvarez, and E. Dagotto, Phys. Rev. B **65**, 241202 (2002).
- ³²S. Das Sarma, E. H. Hwang, and A. Kaminski, Phys. Rev. B **67**, 155201 (2003).